Experimental Model and Immunohistochemical Comparison of U87 Human Glioblastoma Cell Xenografts on the Chicken Chorioallantoic Membrane and in Rat Brains

TADEJ STROJNIK[1], RAJKO KAVALAR[2], TARA A. BARONE[3] and ROBERT J. PLUNKETT[3]

Departments of [1]Neurosurgery and [2]Pathology, University Clinical Centre Maribor, Maribor, SI-2000, Slovenia; [3]Department of Neurosurgery, Roswell Park Cancer Institute, Buffalo, NY 14263, U.S.A.

Abstract. *Background: To study the neuropathology and selected tumour markers of malignant gliomas, an animalglioma model was developed using the implantation of U87 human glioblastoma cells into chick chorioallantoic membrane. The immunohistochemical characteristics were studied and compared with an orthotopic rodent model. Materials and Methods: The U87 cell suspension was inoculated onto the chick chorioallantoic membrane on embryonic day seven and into the brain of nude rats. Brain tumour sections were examined for various known tumour markers by routine haematoxylin and eosin staining and immunohistochemical analyses. Results: The immunohistochemical analyses showed that S100 protein, glial fibrillary acidic protein and synaptophysin expressions, initially present in tissue culture, were lost in both modeìs. Persistent kallikrein, CD68 and vimentin expressions in U87 cells, as well as in both animal tumour models, were detected. The percentage of p53-positive nuclei, which was higher in the tumours grown on the chick chorioallantoic membrane than in rats, did not correlate with the Ki-67 labelling index. Strong cathepsin expression was maintained from the cell culture to both tumour models. CD3-positive cells and numerous leukocytes, but no CD20-positive cells were detected in any of the animal samples, indicating the immunological response of the host to be primarily cellular. Stronger immune reaction for vascular endothelial growth factor in rats correlated with an observed increase in vascular proliferation in these tumours. Conclusion: A simple, fast-growing, cheap and well-defined chick chorioallantoic membrane model of glioma was established, providing a basis for further experimental studies of genetic and protein expression during human glioma tumourigenesis. This model may possibly replace some rodent models for selective studies.*

Correspondence to: Tadej Strojnik, Department of Neurosurgery, University Clinical Centre Maribor, Ljubljanska 5, SI-2000 Maribor, Slovenia. Tel: +386 51 806371, Fax: +386 23324830, e-mail: t.strojnik@amis.net

Key Words: Animal cancer models, chick embryo, rodent model, tumour markers, immunohistochemistry, glioblastoma, cell xenografts.

Malignant brain tumours represent an outstanding problem in human cancer treatment since infiltrative growth enables the disease to evade all forms of control. Diffuse infiltration renders complete surgical resection difficult and contributes to the high incidence of recurrence. Stereotactic biopsies of astrocytomas have demonstrated the existence of tumour cells at considerable distances from the main tumour (1) and it has also been shown that tumour cells are present at a distance greater than 4 cm from the gross tumour (2). There has been little improvement in the glioblastoma multiforme (GBM) survival rate since the 1980s in the United States (3), despite improved microsurgical techniques and introduction of new drugs. Relatively little information about the mechanisms which underlie diffuse local invasion can be obtained from the study of histological sections of human brain tumours (4). To this end, the development of several animal models has provided specific clues about the formation of gliomas. Such animal models are also beneficial for selective molecular and biochemical analysis of tumour markers. Existing GBM models are based on inoculation of glioma cells into rodent brains or the use of transgenic mice (5-7). These rodent models are limited not only by high costs, long experimental duration, variability and major ethical concerns, but also by the difficulty of obtaining morphological data during tumour progression, resulting in large numbers of animals required to obtain conclusive results (8). A reproducible, cheap and fast *in vitro* GBM model would enable researchers and clinicians to gain additional diagnostic (prognostic) information for planning individualised therapies. This would also contribute to a better understanding of brain tumour cell biology and facilitate discovery and validation of new therapeutic targets. The system used in the current study

consisted of a human tumour grown in a xenogeneic host, the chick embryo. A tumourigenesis model, originating from the U87 human glioblastoma cell line, on the chick chorioallantoic membrane (CAM), a densely vascularised extra-embryonic tissue, was developed. A few studies in chick embryos have been undertaken by others, but the primary focus was to demonstrate metastatic potential and not local invasiveness (9-11). This study aimed to compare the expression of various immunohistochemical markers of U87 cells and spheroids in culture and in rat brain with those grown on the CAM membrane. This model, if similarities with *in vivo* human glioma progression are found, has the potential to offer the opportunity to better understand the biology of tumour progression and the possible interference at molecular levels by down-regulating the most relevant factors.

Materials and Methods

U87 glioma cell culture conditions. U87 is a highly malignant anaplastic glioma clone derived from a 44-year-old Caucasian woman and was kindly provided by Tamara T. Lah (Department of Genetic Toxicology and Cancer Biology, National Institute of Biology, Ljubljana, Slovenia). Its *in vitro* and *in vivo* growth characteristics have been described in detail previously (12-14). The cells were grown in plastic 75 cm^2 flasks with Vent Cap (Corning, Acton, MA, USA). The cell lines were routinely maintained in tissue culture medium, consisting of Dulbecco's modified Eagle's medium (DMEM) (Sigma, St. Louis, MO, USA) containing 10% heat-inactivated foetal bovine serum, 2% L-glutamine, penicillin (100 IU/ml) and streptomycin (100 μg/ml). The flasks were kept in a standard tissue culture incubator (100% relative humidity, 95% air and 5% CO_2) (Forma Scientific, USA) and studied daily by phase-contrast microscopy (Euromex, the Netherlands). The culture medium was exchanged twice weekly.

For transplantations, the monolayer of cells in culture was trypsinized (Trypsin-EDTA; Gibco, Invitrogen Corporation, Carlsbad, CA, USA), washed in phosphate-buffered saline (PBS), pH 7.4, (Sigma-Aldrich Cheme, Steinheim, Germany) and suspended in tissue culture medium. The cell number and viability was determined by trypan blue (Sigma-Aldrich Cheme) exclusion in a haemocytometer (Neubauer improved; Labor Optik).

Spheroid cell growth. For spheroid formation, either the U87 cell suspension or the 0.5 mm tumour fragments were put into a 60 mm Ultra Low Attachment Dish (Corning Inc., NY, USA). The Ultra Low Attachment surface is a covalently bound hydrogel layer that is hydrophilic and neutrally charged, preventing cell attachment. Fifteen minutes prior to the addition of either cells or tumour fragments, medium was added to the surface for rehydration, the medium was aspirated and 5 ml of fresh medium were added. Dishes were kept in a standard tissue culture incubator as described above. The spheroids were studied daily by phase-contrast microscopy, for up to 30 days, at which time they were fixed for histology and immunohistochemistry.

Chick chorioallantoic membrane (CAM) model. Fertilised chicken eggs (*Gallus gallus domesticus*) were obtained from a local supplier (Perutnina Ptuj d.d., Slovenia) and kept in a humidified incubator at 37.0˚C and 80% humidified atmosphere. On embryonic day (E) seven, twenty eggs were candled and the outside surface was sterilised with ethanol. After puncturing the air chamber, the shell was thinned under the stereomicroscope with a high speed drill above the CAM near the intersection of major blood vessels. U87 cell suspension ($3\text{-}5\times10^6$ cells in 40 μl of medium) was deposited on the intact CAM and the opening in the shell was sealed with a piece of transparent tape (TESA). On day E 14, eggs were opened, embryos, if alive, were decapitated and CAMs with tumour were excised and fixed in 10% buffered formalin and processed for histological and immunohistochemical analysis.

Nude rat model. The research protocol was reviewed and approved by the Institute Animal Care and Use Committee, Roswell Park Cancer Institute, Buffalo, New York and conformed to the National Institute of Health guidelines. Nude rats (Hsd:RH-Foxn1^{rnu}) originally obtained from Harlan Sprague Dawley Co. (Indianapolis, IN, USA) were bred and maintained in specific pathogen-free conditions. All animal procedures were performed in a laminar flow hood. Three-month-old male nude rats were anesthetised with a ketamine (90 mg/kg) xylazine (4 mg/kg) mixture and placed in a stereotaxic frame (Kopf Instruments, Tjunga, CA, USA). Subsequently, 2.5×10^4 U87 cells in 2.5 μl serum-free DMEM medium were deposited in a procedure outlined previously (15). Sixteen days after tumour implantation, animals were euthanised by CO_2 asphyxiation and perfused transcardially with PBS followed by 10% formalin. Brains were removed and post-fixed in 10% formalin. The brains were then placed into a rodent brain matrix, cut in the coronal plane and processed for paraffin embedding. Thereafter, 5 μm transverse sections were cut and stained with haematoxylin and eosin (H&E) or labelled for the presence of different markers.

Immunohistochemical analysis. Immunohistochemical staining was performed using a standard technique, according to the protocol of the Department of Pathology at the University Clinical Centre Maribor, Slovenia. The U87 cell suspension was centrifuged at 2500 rpm for 15 minutes, the supernatant poured off and the cell sediment resuspended in 0.5% bovine serum albumin (BSA; Serva, Heidelberg, Germany). Smears were fixed in methanol for one hour and then treated with methanol peroxide solution for 15 minutes. Pre-cultured spheroids were fixed in 10% buffered formalin, embedded in paraffin, and 5 μm sections were cut and mounted on glass slides. Deparaffinisation and staining with the antibodies was performed on a Ventana Benchmark XT automatic immunostainer (Ventana Medical Systems, Tucson, AZ, USA) with an EDTA-based retrieval solution (Ventana CC1, Tucson, AZ, USA). An UltraView universal DAB (diaminobenzidine) detection kit was employed (Ventana Tucson). The slides were incubated with the primary antibodies raised against the Ki-67 marker of proliferation monoclonal antibody (MAb) (1:100 dilution), p53 tumour suppressor protein MAb (1:150 dilution), vimentin developmentally-regulated intermediate filament MAb (1:300 dilution), S100 protein, glial and ependymal cells marker polyclonal antibody (PAb) (1:3000 dilution), astrocyte-specific glial fibrillary acidic protein (GFAP) PAb (1:2500), synaptophysin marker of neuroendocrinal function PAb (1:50 dilution), cathepsin B cystein protease MAb (1:100 dilution), cathepsin L cysteine protease MAb (1:100 dilution), CD68 macrophage and microglia marker anti-human MAb (1:100 dilution), VEGF, a potent mitogen, specific for vascular endothelial

cells which may directly stimulate the growth of new blood vessels MAb (1:100 dilution) (16), CD3 most specific T-cell antibody PAb (1:100 dilution), CD20-specific B-cell antibody MAb (1:100 dilution). Leukocytes contain esterase, an enzyme that splits esters into an acid and an alcohol. Esterase stain is able to show leukocyte infiltration within the tumour. Leukocyte esterase presence was demonstrated according to the method of Burstone (17), using naphthol AS-LC acetate as substrate. All antibodies were purchased from DAKO, Glostrup, Denmark except for cathepsins B (clone 3E1) and L (clone N135), both KRKA, d.d., Novo mesto, Slovenia.

The Ki-67 labelling index (LI) and the percentage of p53-positive nuclei was counted on a minimum of ten randomly selected ×40 high-power fields containing representative sections of tumour and calculated as the percentage of cells with positively stained nuclei to total cells. Immunoreactivity for the other brain-associated cell markers listed above was evaluated as negative (–) when no positive immunoreaction was observed within the tumour or endothelial cells, weak (+) when fewer than 30% of the tumour cells were positive, moderate (++) when 30-60% of the cells were positive, and strong (+++) when more than 60% of cells were positive. Twenty representative fields were counted using ×40 magnification.

Slides stained with omission of the primary antibody served as negative controls for Ki-67 and p53 staining. Positive controls for S100 protein, synaptophysin, GFAP, vimentin kallikrein, VEGF (vessels) and cathepsin L (nerve cells) were performed using normal brain sections. Liver tissue sections were used as a positive control for cathepsin B and spleen for the macrophage surface marker CD68 and CD20. Thymus was used as positive control for CD3. Appendix was used as positive control for esterase stain.

Table I. *Immunohistochemistry of U87 cell smears, spheroids and tumour samples.*

Sample markers§	U87 susp (n=5)	Sph (n=3)	CAM (n=5)	Immunosuppressed rats (n=3)	Nude rats (n=3)
Ki-67 LI†	55%	35%	30%	80%	75%
p53‡	40%	10%	50%	10%	30%
Vimentin	+++	+++	+++	+++	+++
S100	++	+	–	–	–
GFAP	++	+	–	–	–
CD3	–	–	+	+	++
CD20	–	–	–	–	–
Synaptophysin	+	+	–	–	–
Cathepsin B	+++	++	++	+++	+++
Cathepsin L	+++	++	+++	++	++
CD68	+++	+++	++	+++	+++
VEGF	–	–	+	++	++
Esterase	/	/	/	/	+++

Susp: Cell suspension; Sph: spheroids; no: number of samples; GFAP: glial fibrillary acidic protein. †Percentage of K-67-positive nuclei (mean value of samples); ‡percentage of p53-positive nuclei (mean value of samples); §immunoreactivity for other brain-associated cell markers listed in the table was evaluated as negative (–) when no positive cells were observed within the tumour, weak (+) when <30% of the cells were positive, moderate (++) when 30-60% of the cells were positive and strong (+++) when >60% of cells were positive.

Results

Macroscopic findings: CAM. Seven days after inoculation (day E 14), 17 out of 20 chick embryos were viable and all showed tumour growth. Area of tumour infiltration ranged from 3 mm^2 to 21 mm^2. Tumour nodules were mostly solid and spherical in shape. Five CAM tumours were more star-like in shape, with spreading of the tumour along the vessels (Figure 1). Tumours were surrounded with a zone of oedema.

Nude rats. In all three rats, a solid, spherical tumour growth with a zone of peritumoural oedema in the ipsilateral hemisphere was observed. Tumour volume ranged from 45 mm^3 to 140 mm^3.

Histopathology: CAM. Within the CAMs blood vessel-rich connective tissue, multiple small tumour nodules were observed (Figure 2). Their size ranged from 0.2×0.3 mm (to 0.8×0.9 mm). Apart from gross tumour mass, small groups of infiltrative tumour cells were seen within the connective tissue and attached to vessel walls. This focal infiltration of neoplastic cells into perilesional tissue was a common finding. In most cases, a narrow band of leukocyte infiltrate, consisting of granulocytes and lymphocytes, surrounded the tumour nodules. The tumour cells were spindle-shaped or polygonal with round or oval hyperchromatic nuclei with nucleoli. They had a tendency to grow closely packed in whorls and streams. Small anaplastic and giant cells were also observed. Necrosis in these tumours was not common (only 20% of cases) and there was no evidence of nuclear pallisading around the necrotic foci. Little endothelial proliferation was seen within the tumour nodules.

Nude rats. All tumours were sharply demarcated against the surrounding brain tissue (Figure 3). There were neither bands of leukocyte infiltrates surrounding the tumour nor any focal lymphocyte infiltration. Within the tumour, polygonal cells were densely packed. The tumours diameter ranged from 5×7 mm to 3×5 mm and irregular with extensive peritumoural oedematous reactions, especially in the white matter of the ipsilateral hemisphere. In the tumour periphery, numerous blood vessels demonstrated tumour neovascularisation. Necrosis in these tumours was not observed at this time point (16 days after inoculation). The full range of cytological features of human glioblastoma was observed in these tumours, including astrocytes, small anaplastic cells, spindle cells and giant cells.

Immunohistochemistry. Results of the immunostaining are summarised in Table I. The index of proliferation, Ki-67 LI, was high in all samples, but the fraction of Ki-67-positive cells was higher in the rat model (Figure 4A) (mean value 75%), compared to CAM (Figure 4B) (30%). In cell suspension and in tumours on CAM, more nuclei stained positively for p53 (Figure 4C) (mean value 50%) compared to tumours in rats (Figure 4D) (mean value 30%). All of the tumour cells

Figure 1. *Tumour nodules were seen on CAM one week after inoculation of U87 cells. Note small satellite tumours apart from the main tumour mass (arrow).*

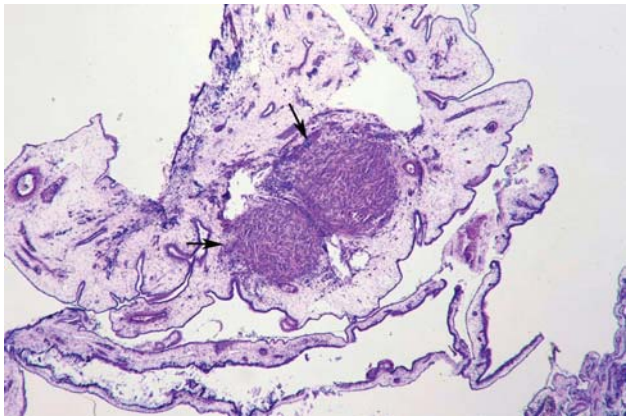

Figure 2. *Within the CAMs, loosely connective tissue with blood vessels two tumour nodules can be seen (arrows) (HE, ×4).*

presented a strong immune reaction for vimentin. Reactive astrocytes, cells of the ependyma, choroid plexus and vascular endothelia were vimentin negative, whereas vessel walls in CAM stained positively for vimentin (Figure 5A). The expression of S100 protein was moderate in the cells in suspension and minimal in the tumour cells of the spheroids. Tumour cells on the CAM and in the rats were S100 negative, whereas strong immunostaining was noted in the surrounding normal and oedematous brain tissue, especially reactive astrocytes. The cell suspension expressed GFAP to a moderate degree; in the spheroids only weak staining was noted, whereas the tumours in chick CAM and in rats were GFAP negative. Normal and oedematous brain tissue showed an intense expression of GFAP in nearly all astroglial cells (Figure 5B). Reactive astrocytes within the peritumoural oedema lesion revealed strong positive immunoreactivity. No CD3-positive cells were observed in cell suspension or in the spheroids, whereas CD3-positive lymphocytes were observed in small numbers in tumours on CAM and especially in nude rats, where more intense lymphocyte T infiltration was seen (Figure 5C). No CD20 staining was observed in any of the samples. Tumour cells in the suspension and in the spheroids expressed weak synaptophysin immunoreactivity, whereas tumours on CAM and in rats were synaptophysin negative. The surrounding brain tissue displayed an intense expression of synaptophysin. Strong immunostaining for cathepsin B was noted in all samples; especially in rats (Figure 5D). Vascular endothelia were also positive for cathepsin B. Staining with the cathepsin L antibody revealed a strong positive reaction in the cells in suspension. The spheroids presented a moderate reaction. The expression of cathepsin L in the tumour cells of the tumours was strong, whereas there was no reaction in the vascular endothelia (Figure 5E). In some tumours, staining was stronger in the centre of the tumour. The cortical pyramidal cells also stained positively for cathepsin L.

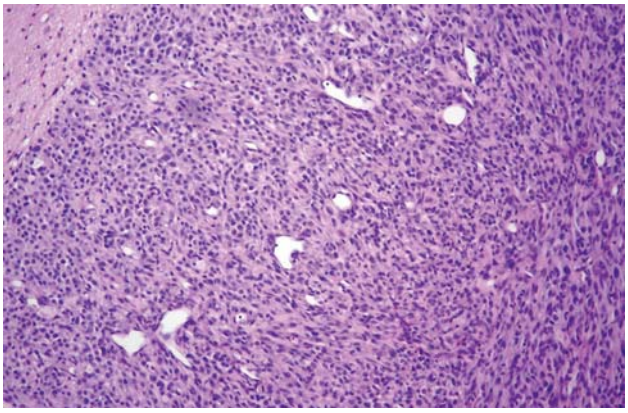

Figure 3. *All tumours in rats were sharply demarcated against the surrounding brain tissue (HE, ×40).*

Staining with the CD68 antibody revealed a strong positive reaction in most of the cells in suspension, spheroids and both animal tumour models (Figure 5F). The tumour periphery, with widespread leukocyte infiltration, showed only weak immunoreactivity for the CD68 antibody, whereas perivascular cell cuffs near the tumour showed a strong positive reaction. There was no expression of VEGF in the tumour cells in suspension or in the spheroids, whereas tumour vascular endothelia displayed a weakly positive reaction. More endothelial proliferation was seen in tumours in rats compared to CAM (Figure 5G). No staining was detected outside the tumour in the rat brains, but some weak staining of the vessels of CAM was detected. In tumours grown on CAM, esterase-positive leukocytes were seen primarily at the tumour margin, whereas in rats, no leukocytes could be observed on the tumour border. However, leukocyte infiltration could be seen inside the tumour (Figure 5H).

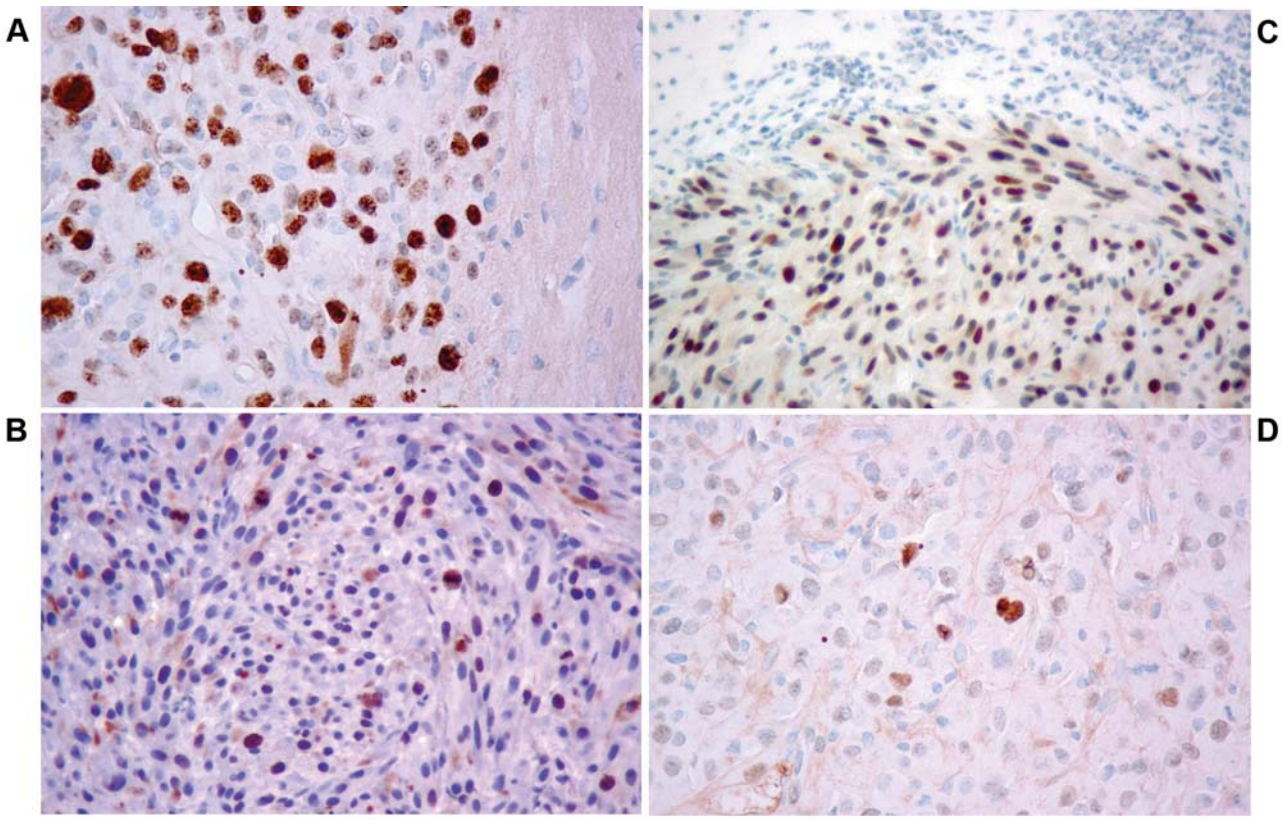

Figure 4. *The index of proliferation, Ki-67 LI, was high in all samples, but the fraction of Ki-67-positive cells was higher in rat brain (×40) (A) than in tumours grown on CAM (×40) (B); more nuclei stained positively for p53 in tumours grown on CAM (×40) (C) than in rat tumours (×40) (D).*

Discussion

The advantages and disadvantages of tumour cell line implantation models of gliomas are well known (18-20). A valid animal model for brain tumours should demonstrate the following characteristics: it must be composed of glial-derived neoplastic cells, the growth rate of the tumour should be predictable and reproducible, the species used should be small and inexpensively maintained, the time to tumour induction should be relatively short, the tumour should have glioma-like intraparenchymal growth and the tumour should also be able to grow in culture (21). The nature of malignant glioma is poorly understood and its study would be facilitated by an *in vivo* model that is easy to manipulate and inexpensive. Current rodent models are limited by high costs, long experimental duration, variability and major ethical concerns. The developing chick embryo CAM was assessed as a xenograft model for the study of human glioma cell lines. The macroscopic tumour appearance, histopathology and immunohistochemistry of selected relevant tumour progression markers were monitored in U87 human glioblastoma cells xenografted on the chick embryo CAM and in the brain of nude rats. The main objective of the current work was to compare the histological and immunohistochemical characteristics of the tumours grown on CAM with an established rodent model.

In accordance with other reports, tumour growth was observed and well established tumours were seen after seven days in the CAM model. There were few differences in histological appearance between tumour models. In both tumour models, the full range of cytological features of human glioblastomas were observed, including astrocytes, small anaplastic cells, spindle cells and giant cells. In rats, tumours were more sharply demarcated from the surrounding brain, while on CAM, tumour nodules grew, with smaller groups of tumour cells growing apart from the gross tumour mass. These cells were usually within the connective tissue with some also attached to the vessel walls. This might be the result of how the tumour cells initially seeded upon inoculation; however, it may possibly mean that this model is more suitable for studying tumour invasiveness. In nude rats, some neovascularisation, especially on the periphery, was detected. A narrow band of leukocyte infiltrate surrounded the tumours grown on CAM but not in nude rats.

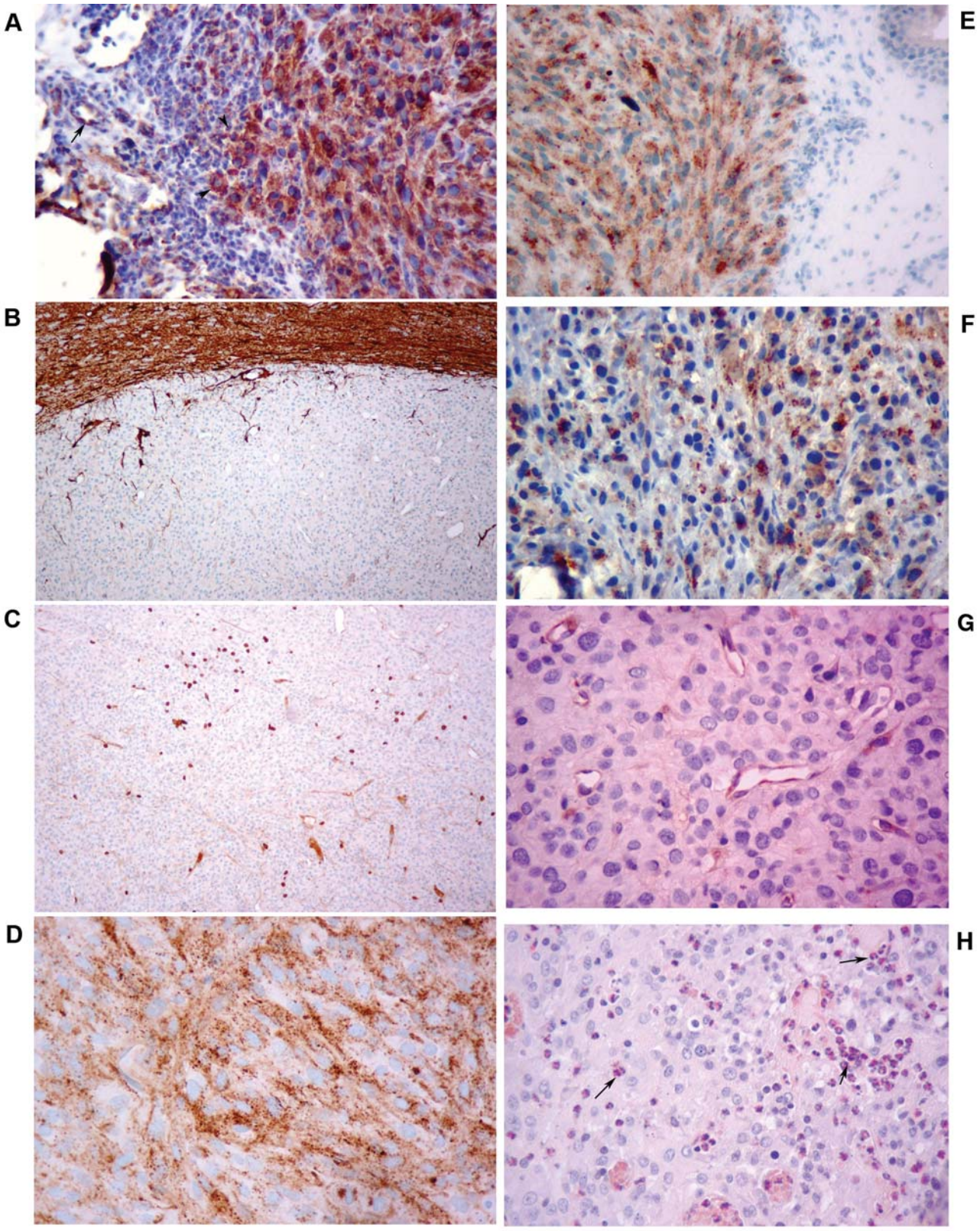
A
B
C
D
E
F
G
H

Ki-67 antigen expression is a measure of the extent of cellular, and hence biological, aggressiveness in malignancy (22, 23). The proliferative activity, defined by Ki-67 LI, has been correlated with progression and prognosis in a number of malignant tumours, including glioma (24, 25). Higher levels of this antigen were found in the U87 cell suspension and in rats compared to the spheroids and CAM tumours, indicating increased proliferation in the rat model.

The *p53* tumour suppressor gene is frequently mutated in glioblastomas (26). Mutations within the *p53* gene often result in aberrant expression of the p53 protein, leading to protein accumulation within the nucleus of the cells. The p53 protein is involved in regulation of the cell cycle and it has been speculated that the presence of abnormal amounts of p53 protein is associated with increased rates of proliferation (25). It was found that the percentage of p53-positive nuclei, which was higher in the tumours grown on the CAM than on rats, did not correlate with the Ki-67 LI. Other workers have also reported little correlation between this pair of immunohistochemical markers (25, 27).

Vimentin is an intermediate filament protein, which marks the mesenchymal cell phenotype. In the course of development of the nervous system, vimentin appears first in immature glial cells (28), but rapidly decreases as GFAP appears concomitantly with myelination (29). In the present work, it was revealed that high production of vimentin by the tumour cells was preserved in the host in both animal models, thus showing that the U87 clone consists of immature cells. Due to strong and specific staining of the tumour cells, it facilitated of visualisation satellite tumours and migrating tumour cells away from the main tumour mass.

GFAP is also an intermediate filament protein and is mostly restricted to mature astrocytes (30). In human malignant gliomas, co-expression of GFAP and vimentin has been reported (31). This was not the case in the animal models used in the current study. Although the U87 cell suspension presented a moderate immune reaction for GFAP, this was completely absent from the induced tumours. This does not necessarily mean that a cell is of non-glial origin, but similarly to that observed for S100, the ability to synthesise GFAP after further dedifferentiation of the U87 cells in the host is gradually lost.

The S100 family of calcium-binding proteins contains approximately 16 members, each of which exhibits a unique pattern of tissue/cell type-specific expression. Although the distribution of these proteins is not restricted to the nervous system, the implication of several members of this family in nervous system development, function, and disease has sparked new interest in these proteins. Different forms of malignant tumours exhibit dramatic changes in the expression of S100 proteins (32, 33). Only moderate S100 immunoreactivity was detected in the U87 cell suspension and weak expression in the spheroids. Tumours in both animal models were S100 negative, which can be explained by the possible down-regulation of S100 expression following tumour dedifferentiation (34).

CD3 is a marker of T lymphocytes. Heterologous transplantation of human tumour cells into animals inevitably leads to immunological response of the host. Cytotoxic T lymphocytes have been implicated as the effectors cell mediating graft rejection (35). Only small numbers of CD3-positive cells were seen in tumours grown on CAM, whereas in nude rats more CD3-positive cells were seen, indicating that some sort of immune response is also present in this immunoincompetent hosts. These CD3-positive cells might be 'T-like' cells, but not actual T-cells, which adopted T lymphocytes phenotype during the dedifferentiation. As expected, no CD3-positive cells were observed in suspension, in spheroids nor outside the tumour.

CD20 is expressed on all stages of B cell development, except the first and the last stages. It is also found on skin melanoma cancer stem cells (36). No CD20-positive cells were detected in any of the models used in the current study. This might be partially explained by the fact that neither B lymphocytes nor antibodies in the circulation nor in the graft itself are required for first-set graft rejection (37).

Synaptophysin is a reliable marker for neurogenic cells. It is an acidic integral membrane glycoprotein of presynaptic vesicles in various neurons and neuroendocrine cells and in tumours derived from such cells (38). Only weak staining was observed in some of the tumour cells in suspension and in spheroids, but no staining was observed in animal tumour models, indicating that tumours induced by U87 clone underwent further dedifferentiation in the host. In humans, pure glial tumours do not usually express synaptophysin.

←

Figure 5. *A: All of the tumour cells presented a strong and specific immune reaction for vimentin, so it was possible to use vimentin staining to visualise satellite tumours and migrating tumour cells away from main tumour mass (arrowheads). Vessel walls in CAM stained positively for vimentin (arrow) (×40). B: Tumours on CAM and in rats were GFAP negative. Normal and oedematous brain tissue showed an intense expression of GFAP in nearly all astroglial cells (×10). C: CD3-positive cells were observed in very small numbers in tumours on CAM and in nude rats where more intense staining was seen (×10). D: Stronger staining for Cat B was noted in tumours in nude rats compared to chicken embryos (×40). E: Stronger staining for Cat L was observed in tumours grown on CAM (×40). F: Staining with the CD68 antibody revealed a strong positive reaction in most of the tumour cells grown on CAM (×40). G: More endothelial proliferation was seen in tumours on rats compared to CAM (×40). H: In tumours grown on CAM, esterase-positive leukocytes could be seen primarily on the tumour margin, whereas in rats, no leukocytes were observed on the tumour border, instead leukocyte infiltration was seen inside the tumour (arrows) (×40).*

Cathepsin B is a member of the lysosomal cathepsin family (Cats), which is comprised of intracellular proteinases of different classes. Malignant progression of human gliomas has been found to be associated with an increase in cysteine proteases (39-42). Cat B expression has been found in tumour cells, macrophages and endothelial cells and the immunostaining of Cat B has been correlated with high histological score and has been significantly associated with poor clinical outcomes (43). As expected, this study found strong staining in culture and in all of the animal models, where not only tumour cells but also endothelial cells stained positively for Cat B. Interestingly, stronger staining for Cat B in tumours was noted in rats than in chicken embryos. This could partially be explained by the relative ease of spreading of the tumour cells in the loose connective tissue of the CAM compared to the brain where more proteolytic activity is needed.

Cat L is also a member of the lysosomal cathepsin family. This study found positive Cat L staining in culture and in all of the animal models. Stronger staining for Cat L in tumours was noted in chicken than in rat embryos. Staining with Cat L antibody revealed strong reaction in tumour cells, but there was no reaction in the vascular endothelia. Cat L immunolabelling in glioma tissue sections was previously demonstrated, where it was mostly localised to the tumour cells and was significantly higher in malignant than in benign gliomas (41). Both Cat B and Cat L activity participate in local brain tumour invasion. However, whereas the level of expression of Cat B in tumour and endothelial cells was found to be prognostic for the survival rate of brain tumour patients, Cat L was not (43, 44). Stronger Cat L staining has been noted in the tumour centre, indicating slightly different roles of both cysteine proteases in local invasiveness and in the malignant transformation of brain tumour cells.

CD68 is a specific marker for resting microglia (45). Tumour cells are occasionally reactive to some macrophage markers (46, 47). Leenstra *et al*. (47) investigated six specimens of cultured astrocytoma cells and reported that nine macrophage markers, including CD68, were clearly reactive in neoplastic astrocytes, whereas astrocytes in normal brain specimens were not reactive. In accordance to quoted studies, this study also found strong CD68 expression in U87 human glioblastoma cell suspension, in U87 spheroids, as well as in rat and chick embryo U87 tumours (48). They stained for CD68 in the same way as macrophages do. Again, only minor differences in CD68 expression between the animal models were noted.

VEGF is a potent mitogen specific for vascular endothelial cells and may directly stimulate the growth of new blood vessels (16). Angiogenesis is induced by tumour cell hypoxia and pro-angiogenetic factors (49). Both brain tumour models showed only low VEGF expression. The slightly higher levels of vascular endothelial proliferation seen in rat tumours may be explained by the likelihood of greater hypoxia associated with larger tumour size It is well known that hypoxia is a potent VEGF trigger.

Leukocyte esterase is an enzyme present in most white blood cells. Neutrophils are present in glioblastoma tissue and not limited to necrotic areas. Fossati *et al*. reported correlation between tumour grade and the extent of the neutrophil infiltration (50). Their role in glioma progression remains unclear. Extensive leukocyte infiltration was observed in the brain tumour models of the current study. This might partially be explained by the fact that xenotransplant acts as a foreign body in both animal models, and perhaps that esterase acts similarly to cathepsins thus contributing to the degradation of extracellular matrix.

Conclusion

In conclusion, the U87 human glioblastoma cell line inoculated onto the chick embryo CAM provides an excellent system for experimental studies of human malignant brain tumours. Data from the comparison of a panel of immunohistochemical markers between the CAM and rat models indicates that tumour protein expression in the CAM model is sufficiently similar to that of the rat model. The Authors believe that the chick embryo CAM model is a good alternative to rodent brain tumour models, and may provide the basis for easier and less expensive multigenetic and multimolecular glioma tumour cell analyses. It also has a potential use in testing individualised therapies.

Acknowledgements

This work was supported by the project P3-0327 granted to T. S. by the Ministry of Higher Education, Science and Technology of the Republic of Slovenia. We thank Professor Dr. Tamara T. Lah from National Institute of biology, Ljubljana, Slovenia, for providing us with the U87 cell line. We also thank Professor Janko Kos, Faculty of Pharmacy, University of Ljubljana, for preparing Cat B and Cat L antibodies.

References

1 Daumas-Duport C, Scheithauer BW and Kelly T: A histologic and cytologic method for the spatial definition of gliomas. Mayo Clin Proc *62*: 435-439, 1987.

2 Silbergeld DL and Chicoine MR: Isolation and characterization of human malignant glioma cells from histologically normal brain. J Neurosurg *86*: 525-531, 1997.

3 Deorah S, Lynch CF, Sibenaller ZA and Ryken TC: Trends in brain cancer incidence and survival in the United States: surveillance, epidemiology, and end results program, 1973 to 2001. Neurosurg Focus *20*: 1-7, 2006.

4 Pilkington GJ, Bjerkvig R, De Ridder L and Kaaijk P: *In vitro* and *in vivo* models for the study of brain tumour invasion. Anticancer Res *17*: 4107-4110, 1997.

5 Dai C and Holland EC: Glioma models. Biochim Biophy Acta *1551*: M19-M27, 2001.

6 Holland EC, Celestino J, Dai C, Schaefer L, Sawaya RE and Fuller GN: Astrocytes give rise to oligodendrogliomas and astrocytomas after gene transfer of polyoma virus middle T antigen *in vivo*. Nat Genet *25*: 55-57, 2000.

7 Reilly KM, Loisel DA, Bronson RT, McLaughlin ME and Jacks T: *Nf1; Trp53* mutant mice develop glioblastoma with evidence of strain-specific effects. Nat Genet *26*: 109-113, 2000.

8 Hagedorn M, Javerzat S, Gilges D, Meyre A, de Lafarge B, Eichmann A and Bikfalvi A: Accessing key step of human tumour progression *in vivo* by using an avian embryo model. PNAS *102*: 1643-1648, 2000.

9 Chambers AF, Wilson SM, Tuck AB, Denhardt GH and Cairncross JG: Comparison of metastatic properties of a variety of mouse, rat, and human cells in assay in nude mice and chick embryos. In Vivo *4*: 215-219, 1990.

10 Chambers AF, Denhardt GH, Wilson SM and Cairncross JG: Malignant properties of P635 glioma are independent of glial fibrillary acidic protein expression. J Neurooncol *11*: 43-48, 1991.

11 Ossowski L and Reich E: Experimental model for quantitative study of metastasis. Cancer Res *40*: 2300-2309, 1980.

12 Fogh J, Wright WC and Loveless JD: One hundred and twenty-seven cultured human tumour cell lines producing tumours in nude mice. J Natl Cancer Inst *59*: 221-226, 1977.

13 Ponten J and Macintyre EH: Long-term culture of normal and neoplastic human glia. Acta Pathol Microbiol Scand *74*: 465-486, 1968.

14 Olopade OI, Jenkins RB, Ransom DT, Malik K, Pomykala H, Nabori T, Cowan JM, Rowler JD and Diaz MO: Molecular analysis of deletions of the short arm of chromosom 9 in human gliomas. Cancer Res *52*: 2523-2529, 1992.

15 Plunkett RJ, Lis A, Barone TA, Fronckowiak MD and Greenberg SJ: Hormonal effects on glioblastoma multiforme in the nude rat model. J Neurosurg *90*: 1072-1077, 1999.

16 Leung DW, Cachianes G, Kuang WJ, Goeddel DV and Ferrara N: Vascular endothelial growth factor is a secreted angiogenic mitogen. Science *246*: 1306-1309, 1989.

17 Burstone MS: Enzyme Histochemistry. New York: Academic Press, 1962.

18 San-Galli F, Vrignaud P, Robert J and Cohadon P: Assessment of the experimental model of transplanted C6 glioblastoma in Wistar rats. J Neuro Oncol *7*: 299-304, 1989.

19 Peterson DL, Sheridan MD and Brown WE: Animal models for brain tumours: historical perspectives and future directions. J Neurosurg *80*: 865-876, 1994.

20 Pilkington GJ and Lantos PL: Pathology of experimental brain tumours. *In*: Neurooncology, Primary malignant brain tumours. Thomas DGT (ed.). London: Edward Arnold, pp. 51-76, 1990.

21 Crafts D and Wilson CB: Animal models for brain tumors. Natl Cancer Inst Monogr *46*: 11-17, 1977.

22 Scott R, Hall P and Haldane J: A comparison of immunohistochemical markers of cell proliferation with experimentally determined growth fraction. J Clin Pathol *165*: 173-178, 1991.

23 Wilson G, Saunders M and Dische S: Direct comparison of bromodeoxyuridine and Ki-67 labeling indices in human tumours. Cell Prolif *29*: 141-152, 1996.

24 Halvorsen OJ, Haukaas S, Hoisaeter PA and Akslen LA: Maximum Ki-67 staining in prostate cancer provides independent prognostic information after radical prostatectomy. Anticancer Res *21*: 4071-4076, 2001.

25 Cunningham JM, Kimmel DW, Scheithauer BW, O'Fallon JR, Novotny PJ and Jenkins RB: Analysis of proliferation markers and p53 expression in gliomas af astrocytic origin: relationships and prognostic value. M/J Neurosurg *86*: 121-130, 1997.

26 Newcomb EW, Madonia WJ, Pisharody S, Lang FF, Koslow M and Miller DC: A correlative study of p53 protein alteration and p53 gene mutation in glioblastoma multiforme. Brain Pathology *3*: 229-235, 1993.

27 Balčiūnienė N, Tamašauskas A, Valančiūtė A, Deltuva V, Vaitiekaitis G, Gudinavičienė I, Weis J and von Keyserlingk DG: Histology of human glioblastoma transplanted on chicken chorioallantoic membrane. Medicina (Kaunas) *2*: 123-131, 2009.

28 Dahl D, Rueger DC and Bignami A: Vimentin, the 57,000 molecular weight protein of fibroblast filaments, is the major cytoskeletal component in immature glia. Eur J Cell Biol *90*: 191-196, 1981.

29 Dahl D: The vimentin-GFAP protein transition in rat neuroglia cytoskeleton occurs at the time of myelination. J Neurosci Res *6*: 741-748, 1981.

30 Lazarides E: Intermediate filaments: a chemically heterogeneous, developmentally regulated class of proteins. Annu Rev Biochem *51*: 219-250, 1982.

31 Herpers MJHM, Ramaekers FCS, Aldeweireldt J, Moesker O and Slooff J: Co-expression of glial acidic protein- and vimentin-type intermediate filaments in human astrocytomas. Acta Neuropathol *70*: 333-339, 1996.

32 Sedeghat F and Notopoulos A: S100 protein family and its application in clinical practice. Hippokratia *12*: 198-204, 2008.

33 Sen J and Belli A: S100B in neuropathologic states: the CRP of the brain? J Neurosci Res *85*: 1373-1380, 2007.

34 Bressler J, Smith BH and Kornblith PL: Tissue culture techniques in the study of human gliomas. *In*: Neurosurgery. Wilkins RH (ed.). New York: Mc Graw Hill, pp. 542-548, 1985.

35 Bierer BE, Emerson SG, Antin J, Maziarz R, Rappeport JM, Smith BR and Burakoff SJ: Regulation of cytotoxic T lymphocyte-mediated graft rejection following bone marrow transplantation. Transplan *46*: 835-839, 1988.

36 Fang D, Nguyen TK, Leishear K, Finko R, Kulo AN, Hotz S, Van Belle PA, Xu X, Elder DE and Herlyn M: A tumorigenic subpopulation with stem cell properties in melanomas. Cancer Res *65*: 9328-9337, 2005.

37 Hall BM, Dorsch S and Roser B: The cellular basis of allograft rejection *in vivo*. J Exp Med 148: 878-889, 1978.

38 Schwechheimer K, Wiedenmann B and Franke WW: Synaptophysin: A reliable marker for medulloblastomas. Virchows Archiv *411*: 53-59, 1987.

39 McCormick D: Secretion of Cat B by human gliomas *in vitro*. Neuropatho Appl Neurobiol *19*: 146-151, 1993.

40 Sivaparvathi M, Sawaya R, Wang SW, Rayford A, Yamamoto M, Liotta LA, Nicolson LA and Rao JS: Overexpression and localization of Cat B during the progression of human gliomas. Clin Exp Metastasis *13*: 49-56, 1995.

41 Rempel SA, Rosenblum ML, Mikkelsen T, Yan PS, Ellis KD, Golembieski WA, Sameni M, Rozhin J, Ziegler G and Sloane BF: Cat B expression and localization in glioma progression and invasion. Cancer Res *54*: 6027-6031, 1994.

42 Mikkelsen T, Yan PS, Ho KL, Sameni M, Sloane BF and Rosenblum ML: Immunolocalization of Cat B in human glioma: implications for tumor invasion and angiogenesis. J Neurosurg *83*: 285-290, 1995.

43 Strojnik T, Kos J, Židanik B, Golouh R and Lah T: Cathepsin B immunohistochemical staining in tumor and endothelial cells is a new prognostic factor for survival in patients with brain tumors. Clin Can Res *5*: 559-567, 1999.

44 Strojnik T, Kavalar R, Trinkaus M and Lah TT: Cathepsin L in glioma progression: comparison with cathepsin B. Cancer Det Prev *29*: 448-455, 2005.

45 Hulette CM, Downev BT and Burger PC: Macrophage markers in diagnostic neuropathology. Am J Surg Pathol *16*: 493-499, 1992.

46 Rossi ML, Hughes JT, Esiri MM, Coakham HB and Brownwell DB: Immunohistological study of mononuclear cell infiltrate in malignant gliomas. Acta Neuropathol *74*: 269-277, 1987.

47 Leenstra S, Das PK, Troost D, de Boer OJ and Bosch DA: Human malignant astrocytes express macrophage phenotype. J Neuroimmunol *56*: 17-25, 1995.

48 Strojnik T, Kavalar R anf Lah TT: Experimental model and immunohistochemical analyses of U87 human glioblastoma cell xenografts in immunosuppressed rat brains. Anticancer Res *26*: 2887-2900, 2006.

49 Hendriksen EM, Span PN, Schuuring J, Peters JP, Sweep FC, van der Kogel AJ and Bussink J: Angiogenesis, hypoxia and VEGF expression during tumour growth in a human xenograft tumour model. Microvasc Res *77*: 96-103, 2009.

50 Fossati G, Ricevuti G, Edwards SW, Walker C, Dalton A and Rossi ML: Neutrophil infiltration into human gliomas. Acta Neuropathol *98*: 349-354, 1999.

Received October 24, 2010
Revised November 13, 2010
Accepted November 16, 2010